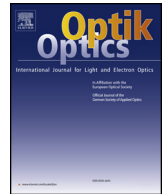




Contents lists available at ScienceDirect

Optik

journal homepage: [www.elsevier.com/locate/ijleo](http://www.elsevier.com/locate/ijleo)

Original research article

# Design and analysis for the flexible support structure of high precision lens assembly

Gao Yan<sup>a,b,\*</sup>, Zhang Bao<sup>a</sup><sup>a</sup> Changchun Institute of Optics, Fine Mechanics and Physics, Chinese Academy of Sciences, Changchun 130033, China<sup>b</sup> University of Chinese Academy of Sciences, Beijing 100049, China

## ARTICLE INFO

## Keywords:

Space telescope  
 Lens flexible support structure  
 Gravity deformation  
 Thermal deformation

## ABSTRACT

In order to achieve support and positioning of lens assembly which have large aperture and high precision in the on-orbit assembly space telescope validation prototype, A novel lens support structure with multi-point flexible units and four point length-adjustable radial holding is proposed. Then, the structure optimization is finished based on gravity deformation and thermal deformation. Finally, the influence of gravity and thermal load on the lens surface figure under this support structure is given by finite element analysis. The results show that: the largest first lens in the lens assembly is taken as an example, lens surface figure (RMS) of the upper surface causing by gravity and +2°C thermal load is 3.09 nm, while the lower surface is 3.03 nm, and lens surface figure RMS of the upper surface causing by gravity and -2°C thermal load is 3.43 nm, while the lower surface is 3.39 nm. The results and practice indicate that the multi-point flexible support structure can effectively reduce the influence on lens surface figure by gravity and thermal load, and can be satisfied with the lens surface figure accuracy (RMS < 4 nm).

## 1. Introduction

With the improvement of high resolution and low aberration performance of optical system and the development of optical manufacturing and integration technology, the requirement of optical elements' surface figure is getting higher and higher, it is necessary to strictly control the lens surface figure under gravity and thermal load. Take the lens assembly which have large aperture and high precision in the on-orbit assembly space telescope validation prototype as an example, the requirements of the lens surface figure (RMS) under using state is better than 4 nm, meanwhile, it requires that the support structure can keep accurate position in shock, vibration, pressure and temperature conditions [1–4]. Therefore, high requirements are put forward for the support structure of optical elements.

Common optical components in optical systems are mainly supported by rigid frames, and pressed by the pressure ring directly. This kind of supporting structure will generate large thermal stress when the temperature changes, and the direct pressure can cause stress birefringence phenomenon in the lens [5–8]. Many scholars have proposed circumferential uniform flexible parts of frame structure. The radial flexible frame structure is studied by Vukobratovich [9], Bacich [10], Bruning [11] and Steele [12] et al. Lens is supported by machining three integrated radial flexible support sheets in the circumferential direction of the lens frame, then use low-stress adhesive to bond the frame and lens [13,14]. Due to the flexibility of the whole frame, the ability of the lens to resist temperature, shock and vibration is effectively improved. However, due to the three-point support used in these radially flexible support structures, the lens needs to undergo a complicated refinement process to remove the tri-leaf aberration introduced by

\* Corresponding author at: Changchun Institute of Optics, Fine Mechanics and Physics, Chinese Academy of Sciences, Changchun 130033, China.  
 E-mail address: [ynogg@163.com](mailto:ynogg@163.com) (Y. Gao).

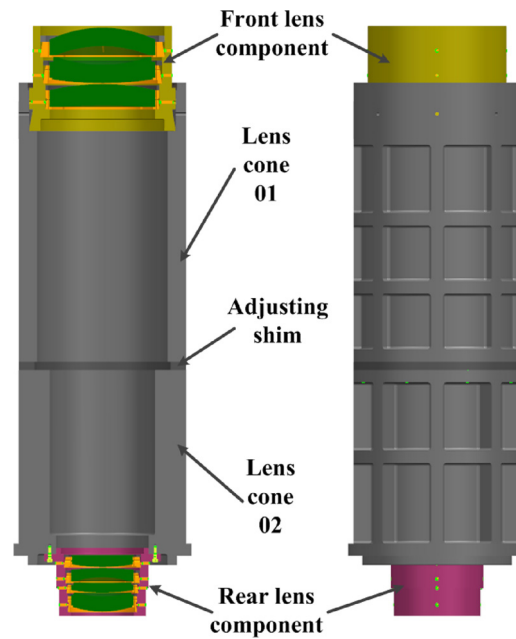


Fig. 1. structure of the lens assembly.

gravity, and the structure will also generate a certain tri-leaf aberration when subjected to thermal loads.

Watson et al. [15] proposed a lens support structure which have a three-point main support, multi-point auxiliary support, and compacts the lens through a compression piece above the main support. However, the structure has a large pressure to prevent the lens from being displaced radially, which causes stress birefringence phenomenon in the lens and even destroys the lens. Sudoh [16] proposed a similar lens support structure which have a three-point main support, multi-point auxiliary support, but compacts the lens above the support points. However, all the supports and pressing pieces are separate structures, which is difficult to install. Moreover, the insufficient radial flexibility of the structure is not good enough to adapt to the thermal deformation of the lens.

In this paper, a multi-point flexible support and an axial four-point adjustable positioning lens support structure is proposed based on lens assembly which have large aperture and high precision in the on-orbit assembly space telescope validation prototype, and the support structure is optimized. Finally the lens surface figure under this support structure is analyzed. The design and analysis method of high-precision lens support structure can provide reference for structural design of other optical instruments.

## 2. Support structure design of lens assembly

The system lens assembly includes seven lenses, structure of the lens assembly includes front lens component, lens cone, adjusting shim, and rear lens component, as shown in Fig. 1. Front lens component have three large aperture lenses, the optical diameter is 171 mm, and the materials of three lenses are N-BK7. Rear lens component have four lenses, the optical diameter is 101 mm. The lens assembly requires very high centering accuracy and air spacing, and the requirement of surface figure accuracy is better than 4 nm. The material of lens cone is Y1Cr13 which have good cutting performance and thermal stability. The entire lens assembly is mounted to a high precision turntable.

The front lens component is mainly composed of lens, frame, adjusting jackscrew, pressure ring and lens barrel. Each lens is mounted in its own frame forming a separate unit, the periphery is bonded with low-stress adhesive D04, and the stress is fully released. The lenses are assembled on different steps in a lens barrel. All the lens units are installed from above and keep a certain gap between the outside diameter of the lens frame and the inside diameter of the lens barrel. The uniform of the lens optical axis is adjusted by adjusting jackscrew. The air spacing and tilt error between the lenses are adjusted by precisely grinding the bottom surface of the lens frame. Finally the pressure ring is pressed tightly. The structure of the rear lens component is the same as the front lens component.

The support structure of each lens unit is shown in Fig. 2, which consists of a lens and a frame with a flexible support structure. The flexible support structure of seven lens units are the same. We take the first lens as an example. The frame has eight flexible supports. The lens is mounted on the lens frame and placed on the support block. Eight injection holes are evenly distributed in the circumferential direction of the frame, and the outer edge of the lens and the frame are bonded with D04 through the injection hole. To ensure that the lens surface deformation is small when the temperature changes, the support material is Y1Cr13 which has similar linear expansion coefficient to the lens material.

The parameters of each lens and its support structure materials are shown in Table 1.

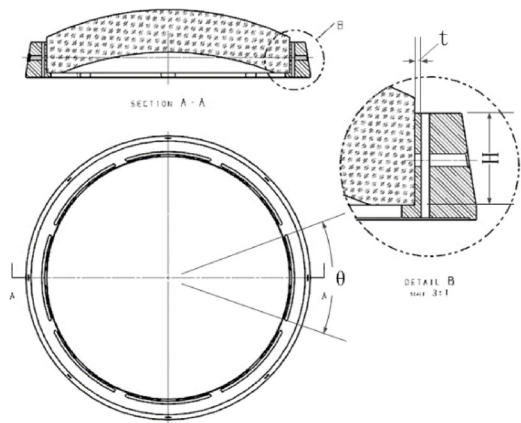


Fig. 2. Flexible support structure of the lens unit.

Table 1  
Material parameters of the structure.

Material	Density $\rho$ (kg/mm <sup>3</sup> )	Modulus of elasticity E(GPa)	Poisson's rate $\nu$	Coefficient of thermal expansion $\alpha$ (10 <sup>-6</sup> /C)
N-BK7	2.52	82	0.206	7.1
Y1Cr13	8.00	193	0.270	9.9
TC4	4.43	114	0.340	8.8
6061	2.68	68.2	0.332	23.6

3. Optimization of the flexible support structure

The accuracy of the optical element's surface figure determines the performance of the optical system, and the installation and positioning of the optical element is a key factor to ensure the surface figure accuracy. Flexible structures are mainly used for supporting and positioning of optical components in optical devices. Optical components, especially large aperture components, require very complex flexible support positioning structures to maintain the position and surface figure accuracy. This is because the flexible structure has a certain flexibility in some degrees of freedom, allowing for a small amount of controllable displacement in this degree of freedom and greater stiffness in other directions. When the ambient temperature changes, the optical element and its support components will be deformed. The mismatch of the thermal deformation coefficient will lead to contact stress. The contact stress will directly affect the surface figure of the optical element and even cause damage, but the flexibility of the flexible structure can effectively reduce the contact stress. The concept of flexible support structure is shown in Fig. 3 [17].

If the lens is directly attached to the frame, the frame deformation will be completely transmitted to the lens. If a flexible structure is set between the lens and the frame, the deformation on the frame can be absorbed. In order to absorb the radial and axial deformation of the lens separately, several flexible units are arranged on the frame. As the number of flexible unit increases, the overall stiffness increases [18]. We select eight flexible supports to ensure sufficient stiffness. Firstly, eight support blocks are machined at the bottom of the lens frame to ensure their coplanarity, and then the slits are cut outside the support block to form a shrapnel with a certain stiffness, which can reduce gravity and thermal influences in the axial and radial directions, as shown in Fig. 4.

All shrapnel is machined on the integral frame by WEDM. The shrapnel will produce axial deformation when supporting the lens. Even if there is an error in the axial direction between the shrapnel, the lens can uniformly act on the shrapnel under the action of gravity, thereby reduces the requirement for high consistency in shrapnel processing. However, when the axial flexibility of the

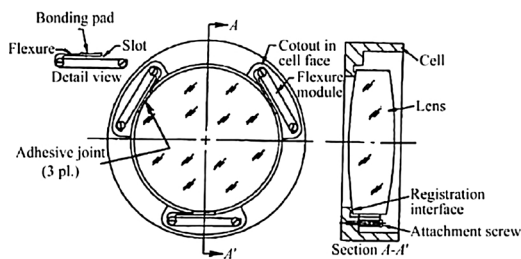


Fig. 3. The flexible support structure concept.

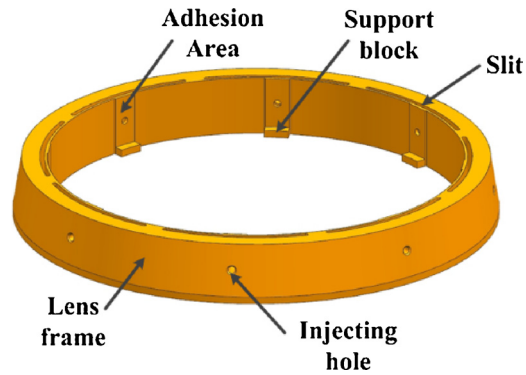
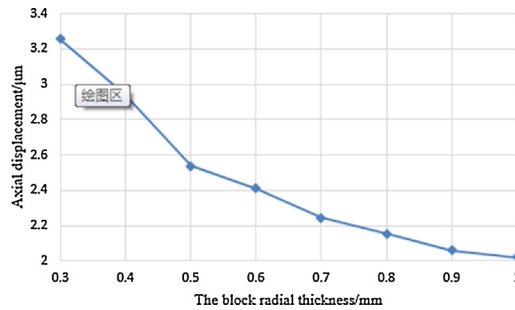
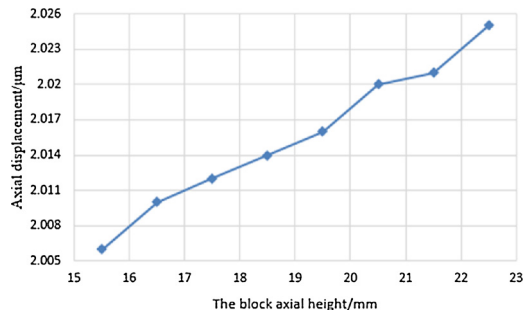
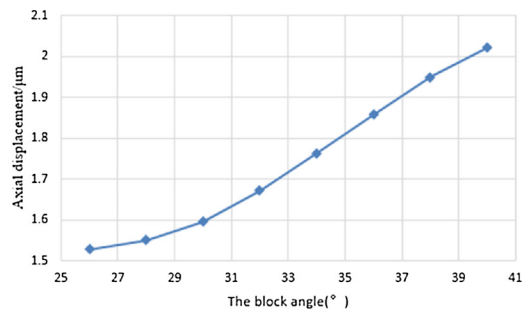


Fig. 4. The flexible lens frame.

Fig. 5. Axis deformation when changing the block radical thickness  $t$ .Fig. 6. Axis deformation when changing the block axial height  $h$ .Fig. 7. Axis deformation when changing the block angle  $\theta$ .

support block is too large, the clamping force of the frame and the feed force of the tool will cause the axial deformation of the support block easily, making the processing technic difficult. The bearing uniformity of each shrapnel can be ensured and the surface figure quality can be improved by reasonably optimizing the size and number of supporting shrapnel structures.

Considering the above factors comprehensively, the axial displacement of the support blocks under the weight of the frame

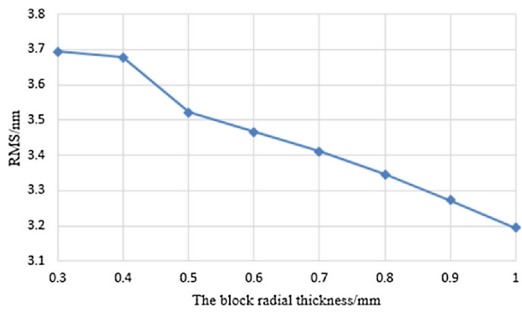


Fig. 8. RMS when changing the block radical thickness  $t$ .

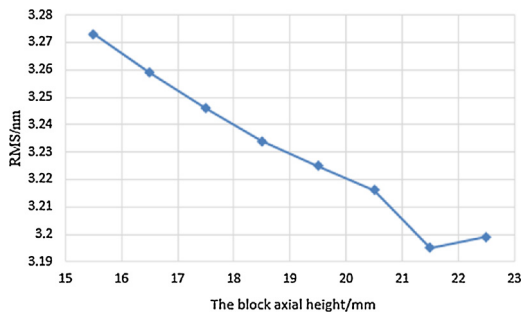


Fig. 9. RMS when changing the block axial height  $h$ .

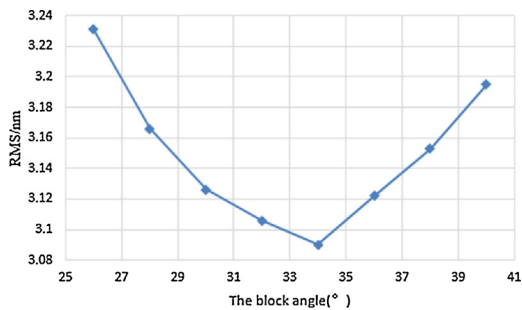


Fig. 10. RMS when changing the block angle  $\theta$ .

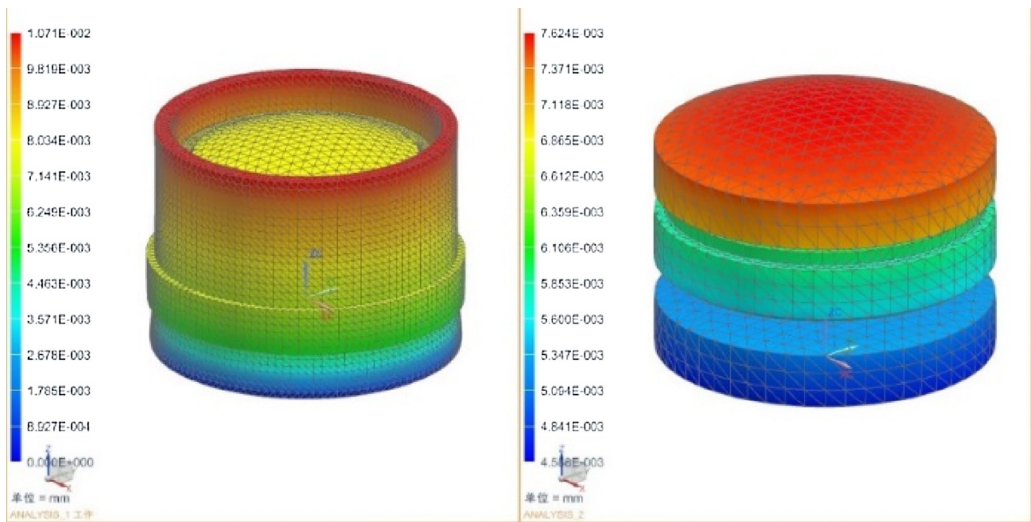


Fig. 11. Deformation contour of the front lens component causing by gravity and + 2°C thermal load.

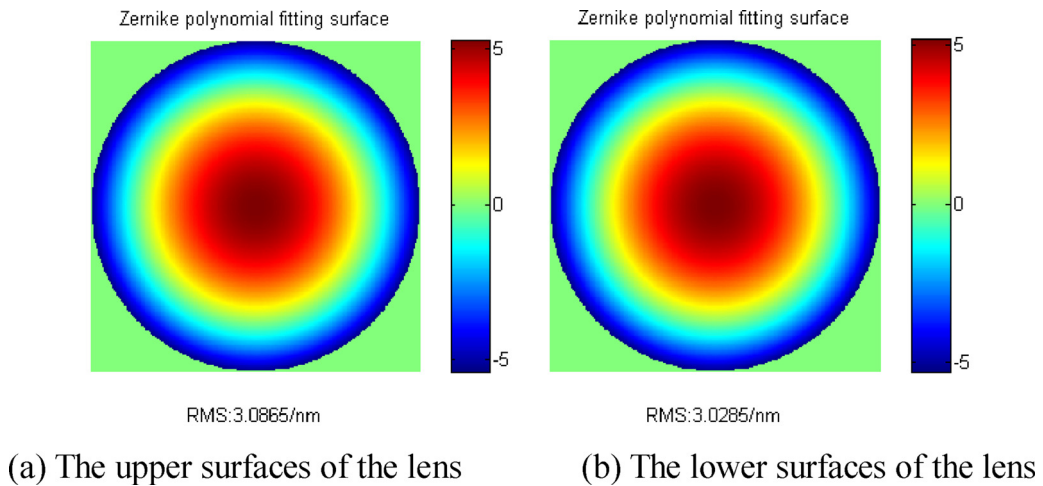


Fig. 12. The surface figure of the lens#1 causing by gravity and  $+2^{\circ}\text{C}$  thermal load.

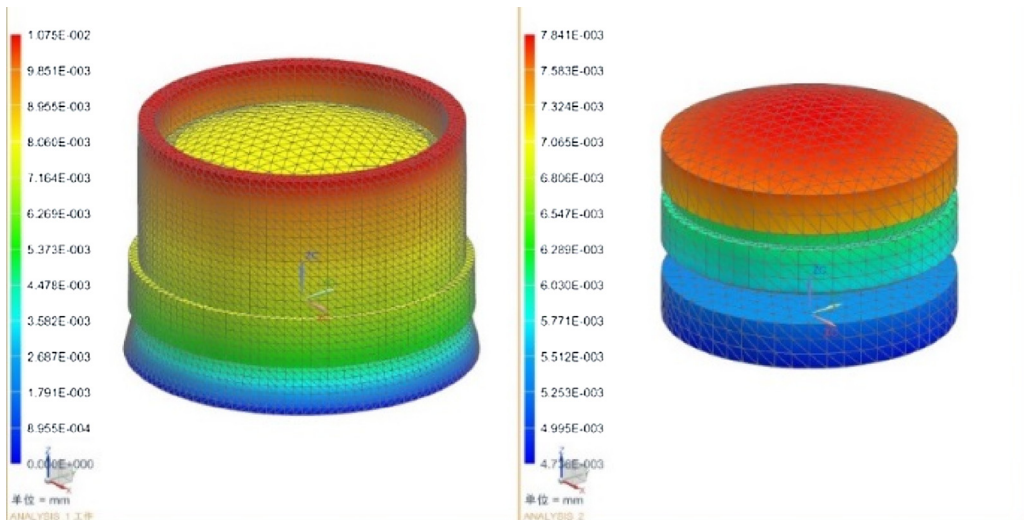


Fig. 13. Deformation contour of the front lens component causing by gravity and  $-2^{\circ}\text{C}$  thermal load.

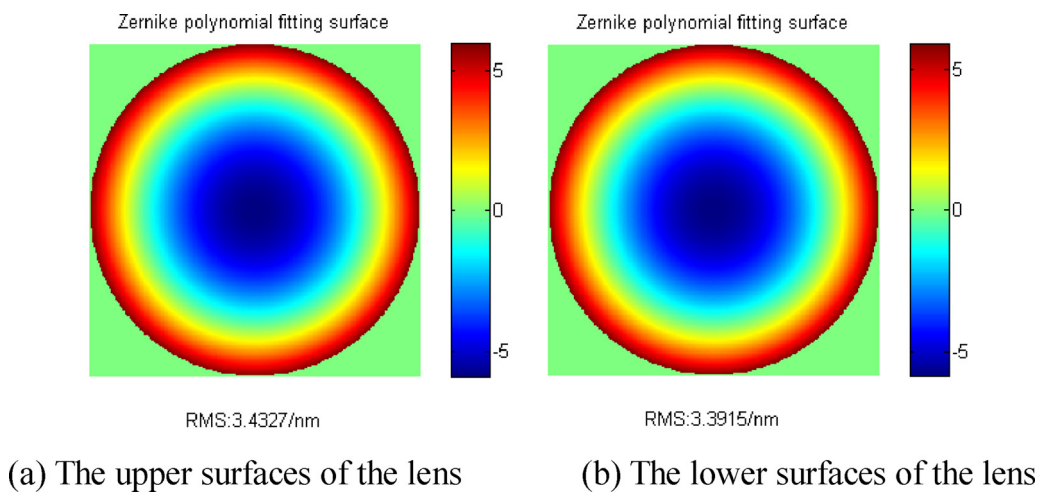


Fig. 14. The surface figure of the lens#1 causing by gravity and  $-2^{\circ}\text{C}$  thermal load.



**Table 2**

The surface figure of the lens component under gravity and + 2 °C thermal load.

	PV(nm)	RMS(nm)
Surf #4(Lens #1 F)	13.74	3.09
Surf #5(Lens #1B)	12.90	3.03
Surf #6(Lens #2 F)	7.47	1.83
Surf #7(Lens #2B)	17.29	1.98
Surf #8(Lens #3 F)	13.90	1.82
Surf #9(Lens #3B)	5.69	0.62

**Table 3**

the surface figure of the lens component under gravity and − 2 °C thermal load.

	PV(nm)	RMS(nm)
Surf #4(Lens #1 F)	14.48	3.43
Surf #5(Lens #1B)	13.32	3.39
Surf #6(Lens #2 F)	5.39	1.24
Surf #7(Lens #2B)	19.92	2.19
Surf #8(Lens #3 F)	12.85	1.88
Surf #9(Lens #3B)	8.90	0.74

**Fig. 15.** The lens assembly adjustment on precision lens eccentric instrument.

assembly is 2  $\mu\text{m}$ . The optimized size parameters are mainly the radial thickness  $t$  of the support block, the axial height  $h$  of the support block and the angle  $\theta$  between the support blocks (Fig. 2).

Fig. 5 shows the axial deformation of support block when the radial thickness  $t$  is taken as 0.3–1.0 mm. The figure shows that the axial deformation decreases with the increase of the radial thickness of the support block. The approximate relationship is a negative exponential function; Fig. 6 shows the axial deformation of support block when the axial height  $h$  is taken as 15.5–22.5 mm. It can be seen from the figure that the axial deformation is proportional to the axial height of support block, but the change is not big; Fig. 7 shows the axial deformation of support block when the angle  $\theta$  between the support blocks is taken as 26°–40°. It can be seen from the figure that the axial deformation increases with the increase of the angle.

Fig. 8 shows the surface figure value of the lens upper surface when the radial thickness  $t$  of the support block is 0.3–1.0 mm



Fig. 16. The lens assembly mounted on the turntable.

respectively. It can be seen from the figure that the surface figure value decreases with the increase of the radial thickness  $t$ . Fig. 9 shows the surface figure value of the lens upper surface when the axial height  $h$  of the support block is 15.5–22.5 mm respectively. It can be seen from the figure that the surface figure value is proportional to the axial height  $h$ , but the influence is not significant. Fig. 10 shows the surface figure value of the lens upper surface when the angle  $\theta$  between the support blocks is  $26^\circ$ – $40^\circ$  respectively. It can be seen from the figure that the surface figure decreases first and then increases with the increase of the angle  $\theta$ , and there is an inflection point.

According to the above analysis, we take  $t = 1$  mm,  $H = 21.5$  mm,  $\theta = 34^\circ$ . At this time, the axial deformation of the lens on the flexible support block is  $1.747\ \mu\text{m}$ , and the RMS of the lens upper surface is  $3.09\ \text{nm}$ , which meets the design requirements.

#### 4. Analysis of the lens surface figure accuracy

The actual support situation of optical components is simulated by NX NASTRAN. The surround surface of the radial injection hole is bonded with the lens, the gravity and thermal load is applied on the component, and the constraint is that the lower reference surface of the lens barrel is completely fixed. The deformation pattern of the component is obtained by solving the finite element model, then the analysis data is subjected to Zernike polynomial fitting to obtain the surface figure accuracy of the lens.

The statics simulation results of the front lens component are shown in Fig. 11. The boundary conditions are the gravity and  $+2^\circ\text{C}$  thermal load. The maximum deformation of the lens is  $7.624\ \mu\text{m}$ , meeting the system requirements. The surface figure of the lens is obtained by analyzing the simulation data on the upper and lower surfaces of the lens, as shown in Fig. 12. The upper surface:  $PV = 13.74\ \text{nm}$ ,  $RMS = 3.09\ \text{nm}$ , the lower surface:  $PV = 12.90\ \text{nm}$ ,  $RMS = 3.03\ \text{nm}$ .

The statics simulation results of the front lens component are shown in Fig. 13 when the boundary conditions are the gravity and  $-2^\circ\text{C}$  thermal load. The maximum deformation of the lens is  $7.841\ \mu\text{m}$ , meeting the system requirements. The surface figure of the lens is obtained by analyzing the simulation data on the upper and lower surfaces of the lens, as shown in Fig. 14. The upper surface:  $PV = 14.48\ \text{nm}$ ,  $RMS = 3.43\ \text{nm}$ , the lower surface:  $PV = 13.32\ \text{nm}$ ,  $RMS = 3.39\ \text{nm}$ .

The surface figure value of lens component are shown in Tables 2 and 3.

According to the above analysis results, the RMS value of each lens meet the optical design index. The lens assembly adjustment on precision lens eccentric instrument is shown in Fig. 15, and the lens assembly mounted on the turntable is shown in Fig. 16. After the installation and adjustment, the surface figure error, tilt error and eccentricity error of the lens assembly all meet the usage requirements.

#### 5. Conclusion

This paper introduces a new multi-point flexible support structure for large aperture lens. Taking the largest and heaviest first lens in the lens assembly (diameter 171 mm, center thickness 30 mm) as an example, the support structure is optimized. The influence of



the flexible support structure on the lens surface figure accuracy is analyzed under gravity and thermal load. The results show that the PV of the upper surface is 13.74 nm, the RMS value is 3.09 nm and the PV value of the lower surface is 12.90 nm, the RMS value is 3.03 nm under gravity and + 2 °C thermal load, and the PV of the upper surface is 14.48 nm, the RMS value is 3.43 nm and the PV value of the lower surface is 13.32 nm, the RMS value is 3.39 nm under gravity and – 2 °C thermal load. Through the analysis results and practice, the multi-point flexible support structure proposed in this paper has good adaptability to large aperture lens support and can meet the surface figure requirements of transmission optical system for large aperture lens.

## Acknowledgement

This research was supported by the program of Research on Key Technology of Ultra Large-aperture On-Orbit Assembly Space Telescope (The program number is 2016YFE0205000), which comes from Ministry of Science and Technology of the People's Republic of China.

## References

- [1] Fulin Chen, Jingxu Zhang, Xiaoxia Wu, et al., Supporting structure of 620mm thin primary mirror and its active surface correction, *Opt. Precis. Eng.* 19 (5) (2011) 1022–1029.
- [2] P.R. Yoder, *Opto-Mechanical Systems Design*, China Machine Press, Beijing, 2008, pp. 191–196.
- [3] Haifeng Peng, Yan Gong, Lei Zhao, Performance index analysis of the support of lithographic lens with multi flexural bracket, *Opto-Electron. Eng.* 40 (2) (2013) 71–75.
- [4] Yangyang Hua, Yan Gong, Design and analysis for the high-precision lens flexible structure of lithography objective lens, *Opto-Electron. Eng.* 40 (7) (2013) 39–43.
- [5] Ping Wang, Bao Zhang, Zhifeng Cheng, et al., Optimal design of cam structure of zoom lens, *Opt. Precis. Eng.* 18 (4) (2010) 893–898.
- [6] Yalin Ding, Haiying Tian, Jiaqi Wang, Design on the focusing mechanism of space remote- sensing camera, *Opt. Precis. Eng.* 9 (1) (2001) 35–38.
- [7] Yifan Wang, Yu Xue, Mechanism design of continuous infrared zoom lens, *Opt. Precis. Eng.* 15 (11) (2007) 1756–1759.
- [8] Xiangyang Sun, Guoyu Zhang, Jie Duan, Investigation of controllable axial conformity for opto-mechanical structure, *Chin. J. Laser* 39 (1) (2012) 0116001-1-0116001-6.
- [9] D. Vukobratovich, Flexure mounts for high-resolution optical elements, *Proc. SPIE (S0277-786X)* 959 (1988) 18–36.
- [10] J.J., Bacich, Precision lens mounting, U.S. 4,733,945 [P]. 1988.
- [11] J.H., Bruning, F.A., Dewitt, K.E., Hanford, Decoupled mount for optical element and attached annuli assembly, U.S. 5,428,482 [P]. 1995.
- [12] J.M. Steele, J.F. Vallimont, B.S. Rice, A compliant optical mount design, *Proc. SPIE(S0277-786X)* 1690 (1992) 387–398.
- [13] Jiasheng Liao, Yan Gong, Wenquan Yuan, et al., Analysis of curing stress magnitude about low stress optical structure adhesives under stable temperature, *Opto-Electron. Eng.* 40 (5) (2013) 138–144.
- [14] Zhihui Wu, Dongping Wang, Liansheng Zhou, et al., Influence of adhesives on dynamics characteristic of opto-mechanical structure, *Opto-Electron. Eng.* 41 (6) (2014) 75–80.
- [15] D. C. Watson, W. T. Novak. Kinematic Lens Mounting with Distributed Support and Radial Flexure [P]. U.S. Patent 6,239,924, 2003-12-25.
- [16] Y. Sudoh. Correction Member, Retainer, Exposure Apparatus, and Device Fabrication Method [P]. U.S. Patent, 6,909,493, 2003-03-14.
- [17] Ahmad, A. and Huse, R. L., Mounting for High Resolution Projection Lense, U.S. Patent 4, 929,054, 1990.
- [18] Yuyan Cao, Zhicheng Wang, Chao Zeng, et al., General modeling optimal design of flexure supporting structure for optical component, *Opt. Precis. Eng.* 11 (24) (2016) 2792–2803.